Int. J. Heat Mass Transfer. Vol. 33. No. 3, pp. 495–506, 1990
Printed in Great Britain

0017–9310/90 $3.00 + 0.00

A study of three-dimensional natural convection in high-pressure mercury lamps—II. Wall temperature profiles and inclination angles

W. SHYY† and P. Y. CHANG‡

† Department of Aerospace Engineering, Mechanics and Engineering Science, University of Florida, Gainesville, FL 32611, U.S.A.
‡ Advanced Technology Department, G.E. Lighting, Cleveland, OH 44112, U.S.A.

(*Received* 9 *January* 1989 *and in final form* 30 *May* 1989)

Abstract—A three-dimensional computational model has been adopted to investigate the natural convection transport of the high-pressure mercury arc discharge in a curved tube. The model solves the combined momentum, continuity, energy, electric field, and simplified radiation transfer equations. The present study investigates the degrees of uniformity of temperature distribution on the tube wall, and the impact of tube inclination angle with respect to gravity on the transport process and the resulting temperature distribution. Good agreements between the predictions and measurements have been obtained. It is found that the gross patterns of gas temperature distribution in mid-plane are rather insensitive to the inclination angle. The wall temperature distribution, however, exhibits substantially greater sensitivity to the inclination angle. This change of characteristics in wall temperature distribution has important effects on the performance of the arctube.

1. INTRODUCTION

IT HAS been well acknowledged that convection plays a very important role in the performance of high-pressure discharge lamps [1–3]. An important requirement for designing a high quality arctube is to distribute the wall temperature as evenly as possible in order to avoid condensation and deposition in the cold regions. The degree of uniformity of temperature distribution, both within the arctube and on the solid wall, can greatly affect the performance as well as the life expectancy of the lamp.

With regard to the transport process of momentum and energy induced by the natural convection, although there are abundant reported results in the literature, both theoretically and experimentally, as evidenced in the voluminous survey conducted by Turner [4] and Gebhart *et al.* [5], very little information is directly available to the present application. The reasons of the sparsity of available information are several. First, the geometry under consideration here is more complicated than the rectangular or annular enclosures that have received most attention by researchers. The electrodes inserted on the two end surfaces of the arctube pose substantially more complexities in the flow field. Second, the present heating source is issued from the electrode discharge, which is embedded in the inner domain of the tube and hence the resulting driving mechanism is different from the conventional problems where heat is transmitted from the bottom surface. Furthermore, the existence of electromagnetic field and radiation heat transfer is important here since the temperature in the arctube typically ranges from several hundred to around several thousand Kelvin.

A three-dimensional convection and thermal computer model has been developed to facilitate this type of investigation [6, 7]. For horizontal high-pressure mercury lamps, a parametric study [7] on geometrical parameters such as curvature and diameter of the arctube, offset and insertion length of the electrodes, and so on has been conducted.

In ref. [7], the focal points were placed on the investigation of the temperature distribution and associated convection pattern in the gas phase while the wall temperature was considered as uniform. Although the transport processes have been well identified in ref. [7], the critical information of temperature distribution on the arctube wall was not available. Here, we have conducted further work on the computational model to yield the information with regard to the wall temperature. Nevertheless, it is found that the overall convection pattern and the qualitative trend in the gas phase established in ref. [7] are very consistent with those found here. The other important aspect studied here is related to the inclination angle of the arctube. This aspect has a very relevant implication in practical mounting of the lamp.

The model enhancements and the theory/data comparison are presented and discussed in the following sections.

2. GEOMETRY OF THE ARCTUBE

Previous investigation [7] has shown that curving the arctube and offsetting the electrodes are the most effective factors in obtaining a desirable temperature distribution within a horizontal high-pressure mercury arctube.

The geometry of the arctube adopted in the present

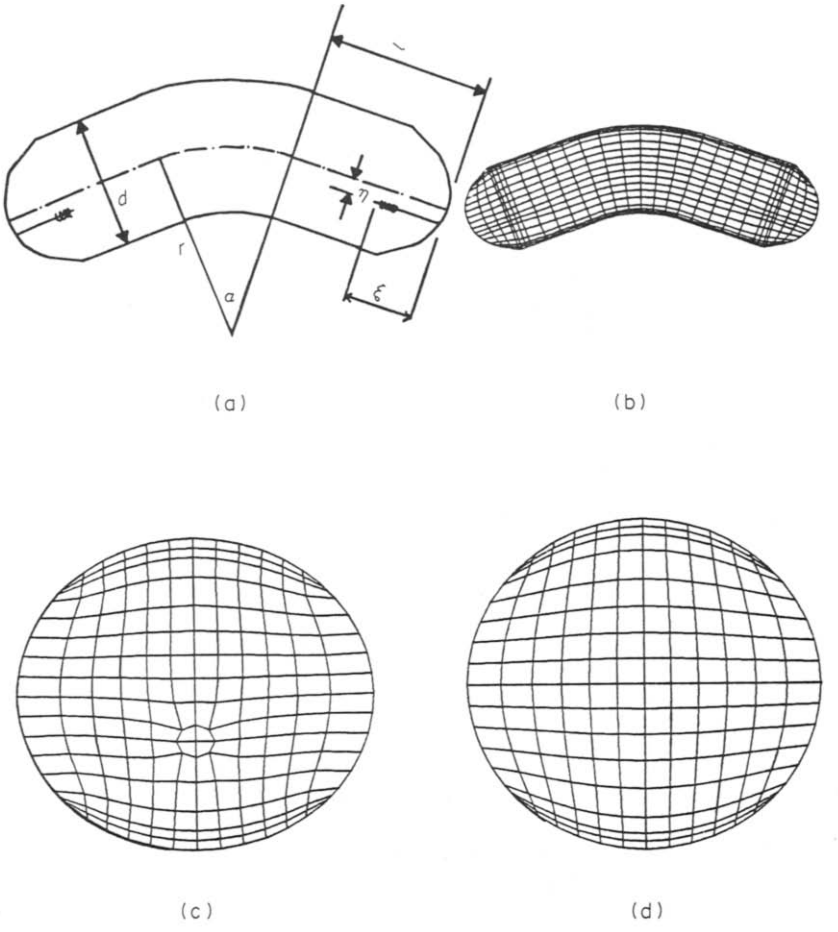

FIG. 1. (a) Arctube design with symmetrical bowl ends. (b) The corresponding computer generated geometry and mesh. (c) Mesh of a cross-section containing the electrode. (d) Mesh of the mid-cross-section.

study is somewhat different from the one adopted in ref. [7]. This change is a reflection of the design evolution of the present lamp. Also in this study, two grid lines have been inserted near the top and bottom walls respectively in regard to the adopted mesh in ref. [7]. This local grid refinement improves the numerical accuracy of the wall temperature prediction. The schematic drawing of the arctube as well as the grid distributions ($29 \times 17 \times 13$) on the side-view and cross-view planes are shown in Fig. 1. Further increasing the number of grids to $29 \times 29 \times 29$ with several grid distributions shows that the maximum changes of temperature at the top and bottom walls are less than 20 and 50 K, respectively. Figure 2 shows the mesh and the offset electrodes in three-dimensional perspectives. Table 1 shows the geometric input data for the arctube used in this study. The input power and mercury pressure are 400 W and 2.5 atm (unless indi-

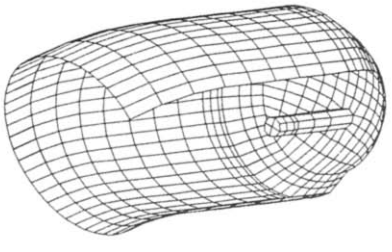

FIG. 2(a). Half of the arctube with the front wall removed (in three-dimensional perspective).

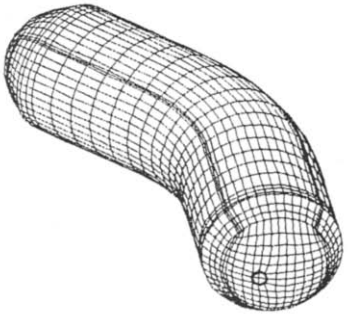

FIG. 2(b). Computer generated geometry and mesh (in three-dimensional perspective).

Table 1. Model input

Symbol	Geometric design parameters	400 W curved arctube model data
d	arctube diameter (mm)	15.1
l	arctube length (mm)	59.3
ξ	electrode insertion length (mm)	9.3
η	offset electrode distance (mm)	2.3
r	radius of bend (mm)	25.4
α	angle of bend (deg)	40
t	wall thickness (mm)	1.2

cated otherwise), respectively. The temperature-dependent fluid properties are taken from Zollweg [2] for the case of a 3 atm discharge in mercury. For variations in mercury pressure, the mercury density is taken to be linearly proportional to the mercury pressure.

For horizontal operation, there are two symmetrical planes. One is the side-view as shown in Fig. 1(b), the other is the mid-plane of the circular cross-sectional view.

3. WALL TEMPERATURE CALCULATION

In ref. [7], the wall temperature was assumed to be uniform. In the present study, the temperature distribution of the quartz inner wall is determined by the energy balance, equation (1), at the gas–wall boundary, which consists of three terms: energy conducted to the wall by the gas, radiant energy absorbed by the wall, energy conducted through the arctube wall. The temperature distribution of the quartz outer wall is determined by the energy balance, equation (2), at the arctube outer boundary, which consists of two terms: energy conducted to the outer boundary through the wall thickness and energy radiated by the wall. The above mentioned terms are formulated as follows:

energy (per unit area) conducted to wall by gas

$$-k_{\text{gas}}\frac{T_{\text{w}}-T_{\text{P}}}{\delta}$$

radiant energy (per unit area) absorbed by wall

$$C\cdot R$$

energy (per unit area) conducted through wall thickness

$$-k_{\text{qtz}}\frac{T_{\text{qtz}}-T_{\text{w}}}{t}$$

energy (per unit area) radiated by wall

$$\sigma\varepsilon(T_{\text{qtz}}^4-T_{\text{sink}}^4)$$

$$-k_{\text{gas}}\frac{T_{\text{w}}-T_{\text{P}}}{\delta}+C\cdot R=-k_{\text{qtz}}\frac{T_{\text{qtz}}-T_{\text{w}}}{t} \quad (1)$$

$$-k_{\text{qtz}}\frac{T_{\text{qtz}}-T_{\text{w}}}{t}=\sigma\varepsilon(T_{\text{qtz}}^4-T_{\text{sink}}^4) \quad (2)$$

where k is the thermal conductivity which is a function of temperature, T the temperature in Kelvin, P the center of a control volume, w the quartz inner wall, δ the normal distance from the center of the fluid control volume to the wall, C the fraction of radiation impinging on the wall which is absorbed, R the radiation impinging on the wall per unit area, qtz stands for quartz, T_{sink} the outer jacket wall temperature, t the quartz wall thickness, σ the Stefan–Boltzmann constant, and ε the quartz emissivity which is a function of temperature.

Order of magnitude analysis indicates that as far as conduction in the wall is concerned, the radial direction is the only dominant one. Conduction along both the longitudinal and circumferential directions of the wall is negligible.

An accurate treatment of 'radiant energy absorbed by the wall' is a difficult task due to the irregular three-dimensional geometry and the moving hot arc position during iterative calculation. The fraction of radiation impinging on the wall which is absorbed is also difficult to determine. Theoretically it depends on wavelengths as well as on temperature. To obtain an approximate treatment of this term, view factors from the hot arc to the inner wall were calculated from the software RAVFAC, documented in a NASA contractor report [8]. The geometry of the curved arctube was treated as a cylinder with flat end caps and the hot arc considered as a much smaller concentric cylinder between the electrode tips within the arctube as shown in Fig. 3. This radiative absorption of the wall is assumed to be 10% in the model calculations.

Both measurements and calculations of the outer quartz wall temperatures were conducted with a

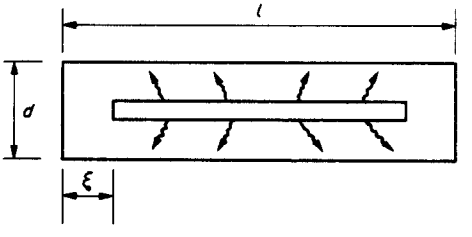

FIG. 3. Schematic drawing of arctube geometry used to calculate view factors (refer to Table 1 for l, d, ξ).

vacuum outer jacket so that the convection effect outside the arctube is not present.

4. EXPERIMENTAL MEASUREMENTS

Both direct photographs of operating arctube and measurements of wall temperature have been made to facilitate assessment of the predictions of the present model. The quartz wall temperature measurements were made with an Ircon-series-7000 radiation pyrometer, an optical device which can quantitatively measure the radiance of a blackbody or other radiating object. Several mercury arctubes of slightly varying mercury doses with vacuum outer jackets were measured. Aquadag was applied on the locations where the temperature measurements were intended. Each aquadag spot was about 2 mm in size and was opaque. To take measurements, the optical head position was adjusted to sight on an aquadag spot at normal incidence. Then the radiant measurements obtained from the radiation pyrometer were converted and calibrated to degrees Centigrade.

5. RESULTS AND DISCUSSIONS

Based on the computed flowfield, an estimation can be made for the Grashof number, which is the measure of the relative importance of the buoyancy force and the viscous effect

$$Gr = \frac{gd^3\Delta\rho}{\nu^2\rho} \tag{3}$$

where g is the gravitational acceleration, d the arctube diameter, ρ the density of mercury gas, and ν the kinematic viscosity of mercury gas.

The formula adopted for computing the dynamic viscosity of mercury gas, μ, is

$$\mu = 2.4789\times10^{-5} + 7.64\times10^{-8}T + 1.039\times10^{-3}\exp\left(-\frac{1.4867\times10^{4}}{T}\right) \tag{4}$$

with the unit of kg m^{-1} s^{-1}, where T is the gas temperature in Kelvin. It is also noted that the Prandtl number is taken as a constant value of 0.56. As to the equation of state under the constant pressure of 2.5 atm, the following formula is adopted:

$$\rho = A/T + B \tag{5}$$

where $A = 5.9353\times10^{3}$ kg m^{-3} K and $B = -0.0465$ kg m^{-3}.

5.1. *Horizontal arctube*

Based on the computed flowfield and temperature contours, it is estimated that the Grashof number is of the order of 10^5, and hence the flow is in the laminar regime but contains a substantial convective effect.

Figure 4(a) indicates the locations where the calculated and measured data of the wall temperature are compared. Figure 4(b) compares the calculated and measured top wall temperatures while Fig. 4(c) compares the calculated and measured bottom wall temperatures. The unsymmetric profiles of the measurement indicate the degree of experimental inaccuracy.

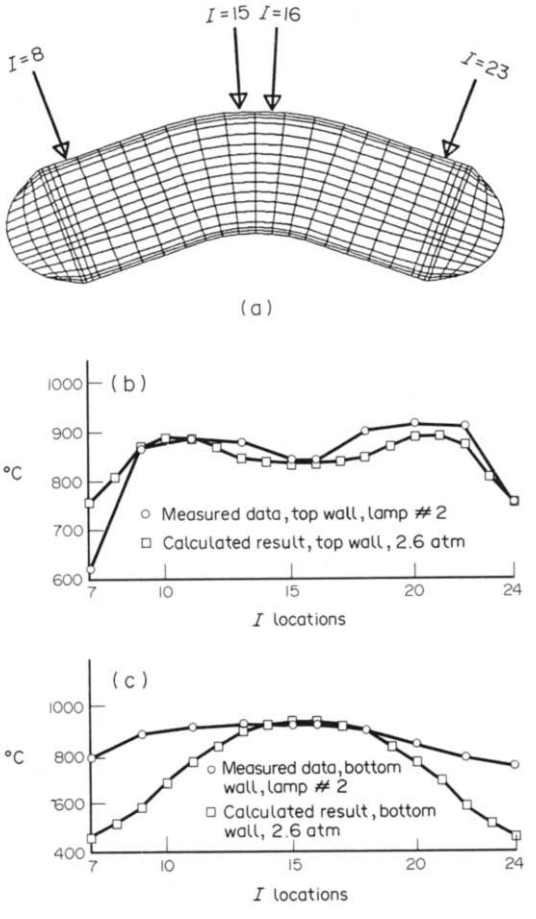

FIG. 4. (a) The I locations in the central plane where the measured and calculated data are compared. (b) Temperature profiles of the top wall in the central plane. (c) Temperature profiles of the bottom wall in the central plane.

The calculated top wall temperature profile agrees well with the measured data. It is observed that the curving of the arctube causes the profile to show a double peak. For the bottom wall temperature, on the other hand, the curving causes the profile to show a single peak at the center. These characteristics result from the interaction of the upward buoyancy effects of the temperature contours and the bending of the arctube shape. It is noted that in the arctube, the highest temperature appears in regions near the two electrode tips. Between the electrodes, there is a current strip along the axial direction where the temperature is higher than in other regions. The curvature of the strip is a product of the balance of the buoyancy effect, which tends to push the higher temperature gas upward, and the electric field effect, which tends to minimize the length of the strip to maintain the continuity of the electric current. It is clear that, in order

to yield the uniform wall temperature distribution, the optimal design of an arctube with a given power input should accommodate the wall curvature to the curvature of the high temperature strip between the electrodes. The curvature of the high temperature strip results from the balance of competing effects of the buoyancy and the electric field. With this physical picture in mind, the results presented in Fig. 4 suggest that in view of the double-peak temperature profile, the curvature along the top wall of the present arctube may be too high.

The calculated bottom wall temperature agrees well with the measurement in the center region but there is quite a discrepancy outside this region. The discrepancy is possibly caused by the following factors.

(1) The tungsten electrodes are much hotter than the wall; therefore, conduction from the electrodes will heat up the end wall regions. However, this is not taken into account at the present time.

(2) The surfaces of the tungsten electrodes are much hotter than the inner quartz wall; therefore, the radiant energy exchanges between these two surfaces would increase the quartz inner wall temperature, especially the regions around the electrodes. This is rather difficult to account for in the context of the simplified treatment of radiation heat transfer adopted here.

(3) The steady-state temperature distributions show that the bottom wall would absorb more radiant energy from the hot arc than the upper wall. But the approximate treatment of 'radiant energy absorbed by the wall' makes no distinction of positions around the circumferential boundary.

Each of these items would raise calculated temperatures in the end wall regions, and/or the bottom wall. These factors will be considered in a future study.

5.2. *Inclination angle*

Next, we turn our attention to the effect of inclination angle of the arctube on the convection pattern and temperature distribution. Three different angles, namely, 0° (horizontal mounting), 30°, and 60° have been studied. Here, referring to Fig. 1(a), the tube is inclined by fixing the left end position and tilting the tube to the designated angle. The gross pattern of the gas temperature distribution in the mid-side-view plane of the arctube seems rather insensitive to the inclination angle, as evidenced in Figs. 5–7, where both the direct photographs of the arctube and computed gas temperature contours in the mid-plane are shown for three different inclination angles. A favorable comparison of the visualized temperature patterns between predictions and photographs are demonstrated in Figs. 5–7. It is clear from Figs. 5–7 that the constraint imposed by the electric field equation is dominant in determining the qualitative temperature pattern of mercury gas. The reason of the dominance of electric field is due to the fact that the transport process of heat and momentum is produced by the externally imposed voltage drop between two electrodes in the first place. Hence the buoyancy effects can only modify the shape of the high-temperature core in relatively mild manners. The major changes appear to be in lifting the hotter gas in the upper region of the tube, hence thickening the luminous zone there.

Even though the qualitative pattern of mercury gas temperature in the arctube is not very sensitive to the inclination angle, the wall temperature distribution of the arctube can still show considerable variations with respect to the inclination angle. The change of the relative angle between the arctube geometrical direction and gravity direction causes the characteristic length in equation (3), and hence the Grashof number, to change. Moreover, the effective geometry within which the natural convection takes place also change due to different inclination angles. Figure 8 shows the velocity vectors in the mid-plane along the side-view direction for the cases of 30° and 60° mounting angles. It is clear that there are considerable changes in flow directions as the inclination angle varies. While the buoyancy effect causes the gas velocity to form similar secondary flow patterns with different inclination angles, the relative angles between the velocity vectors and top/bottom walls change substantially. The convection effect modifies the heat transfer rate to the wall as the arctube is tilted, shifting the levels as well as the locations of the highest and lowest wall temperature. Figures 9–11 show the computed wall temperature distribution, both in the two-dimensional projection and in the three-dimensional perspective view, of the arctube with three different inclination angles of 0°, 30° and 60°. Substantial variations in wall temperature distribution can be observed. With the horizontal mounting of the arctube, the wall temperature distribution is symmetric with respect to the mid-cross-sectional plane. As already discussed previously, there are two peak values of temperature on the top wall and one peak value on the bottom wall for the present configuration and operating conditions. With the 30° inclination, the temperature distribution becomes asymmetric, and on both the top and bottom walls there is only one peak value. The temperature distribution becomes more asymmetric as the arctube is inclined at 60°. It is also observed that the overall uniformity of the wall temperature distribution worsens with increasing inclination. The computed highest and lowest values of wall temperature with three different inclination angles are, respectively, 904 and 363°C with 0° inclination, 943 and 331°C with 30° inclination, 1087 and 317°C with 60° inclination. Hence the inclination angle exhibits strong influence on the wall temperature distribution.

6. SUMMARY AND CONCLUSIONS

Based on the results presented in the present study, the following conclusions can be made.

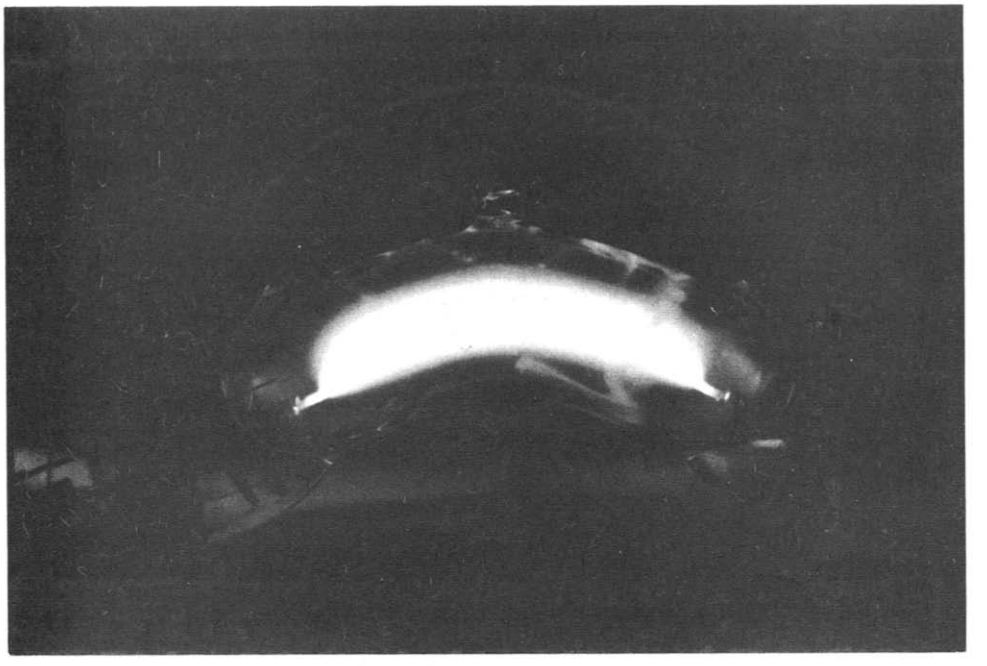

direct photograph

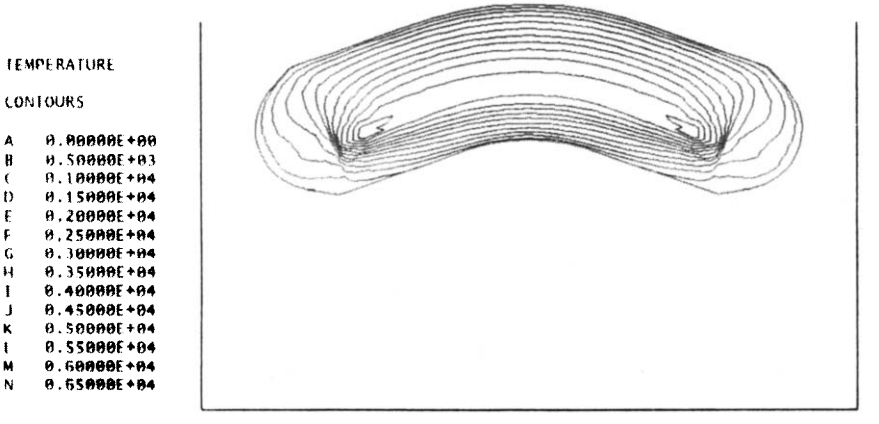

Numerical prediction in mid-plane

FIG. 5. Visualization and temperature distribution of horizontal arctube.

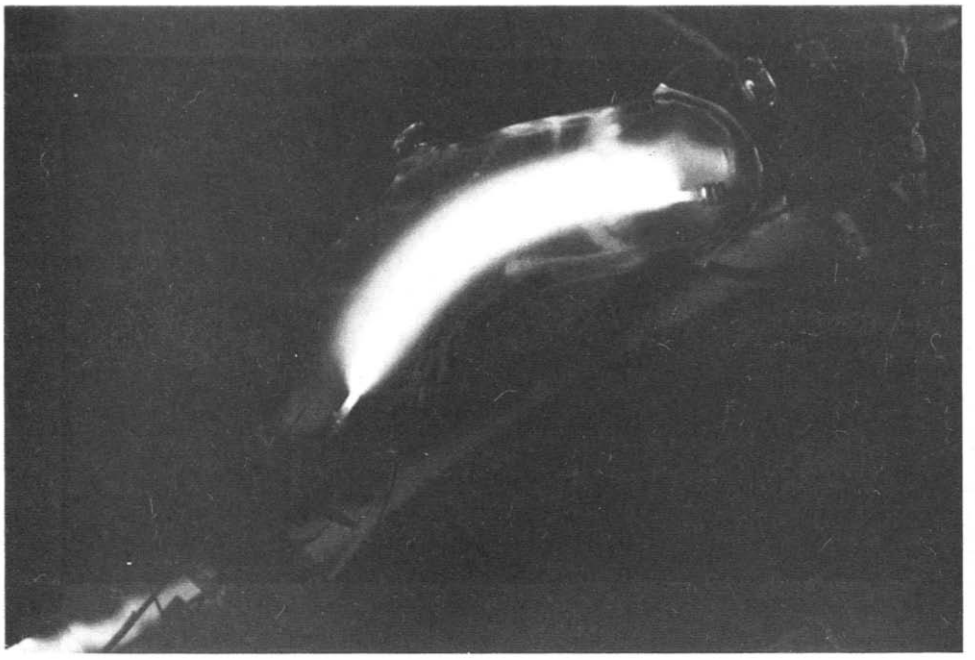

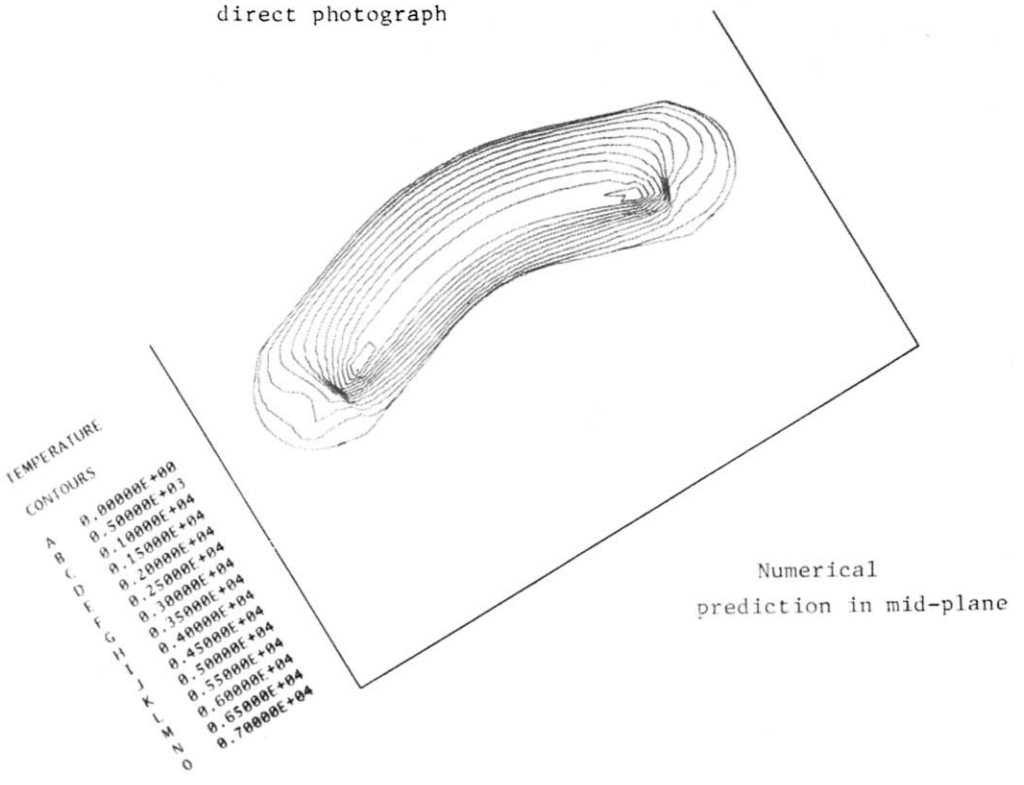

FIG. 6. Visualization and temperature distribution of arctube with 30° inclination.

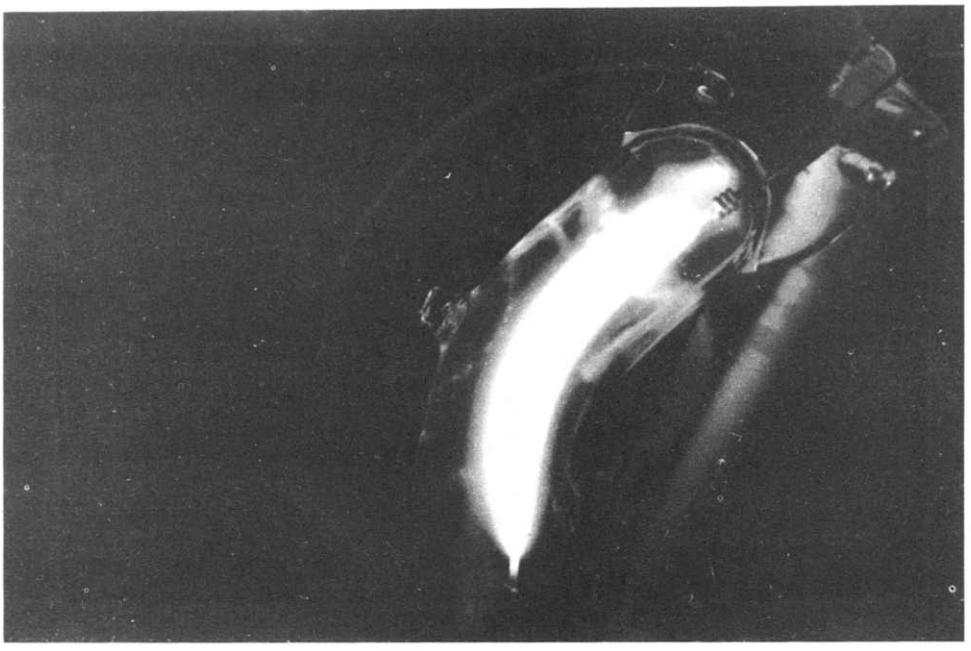

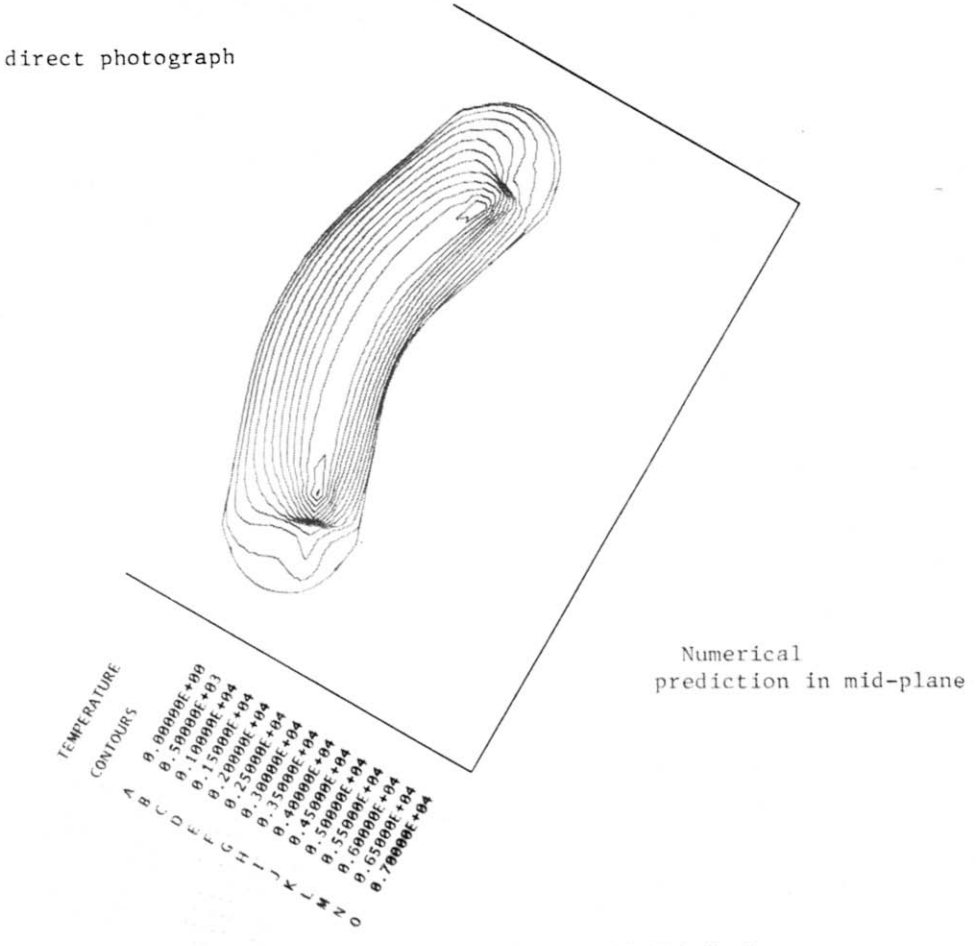

FIG. 7. Visualization and temperature distribution of arctube with 60° inclination.

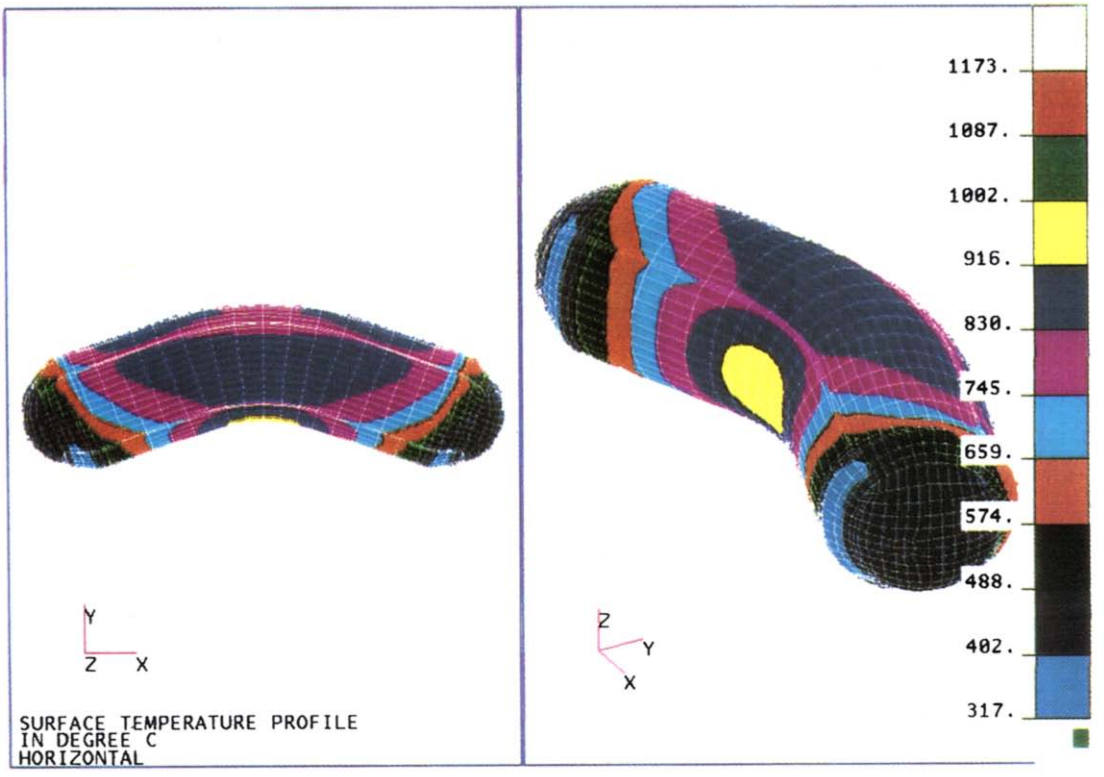

FIG. 9. Horizontal arctube. Wall temperature distribution in two-dimensional projection (left) and three-dimensional perspective (right).

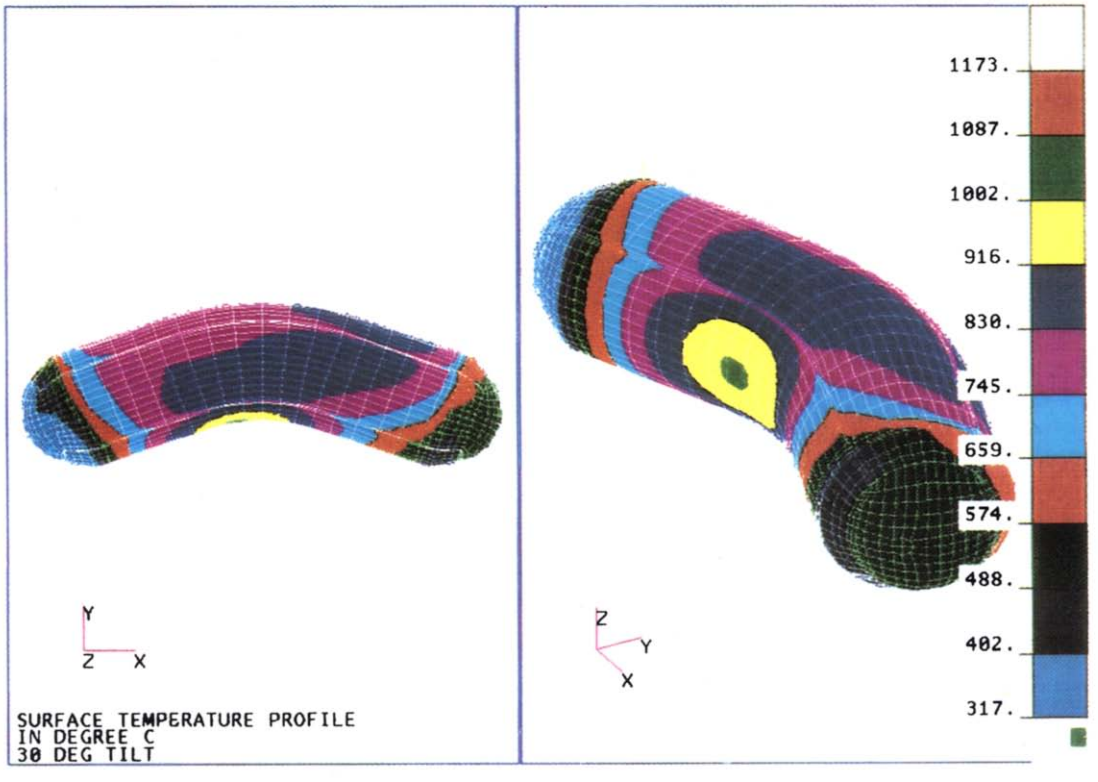

FIG. 10. 30° inclination. Wall temperature distribution in two-dimensional projection (left) and three-dimensional perspective (right).

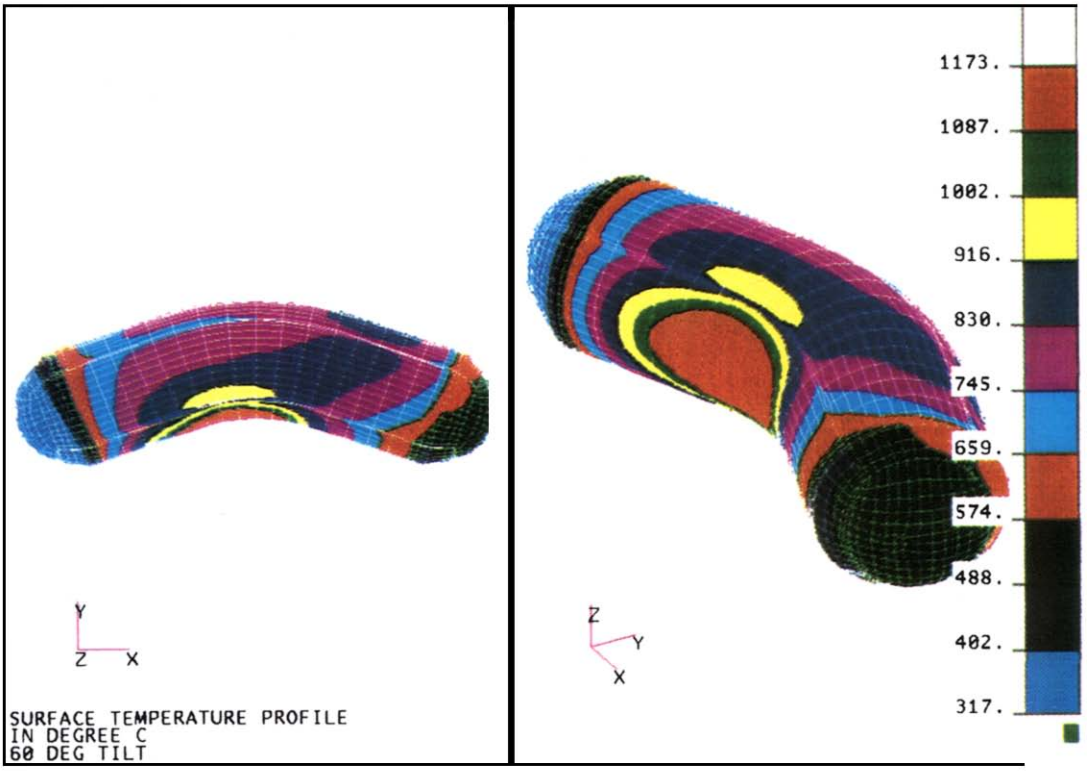

FIG. 11. 60° inclination. Wall temperature distribution in two-dimensional projection (left) and three-dimensional perspective (right).

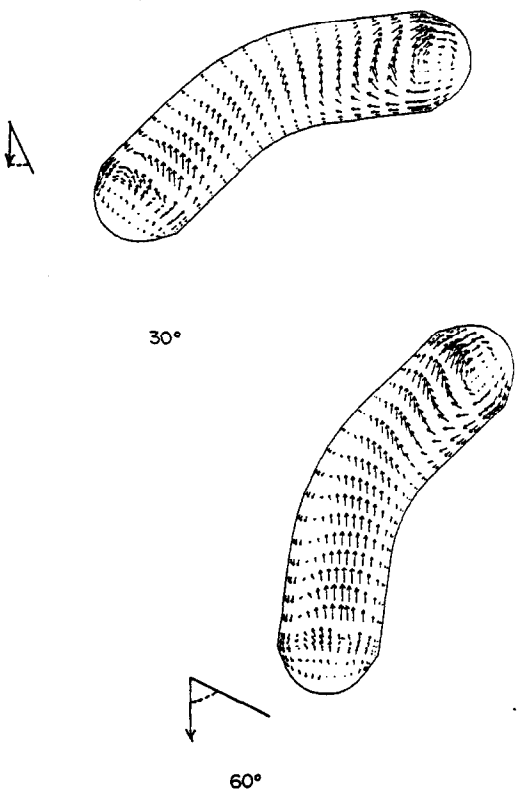

FIG. 8. Velocity vectors in middle side-view plane with two different inclination angles.

(1) Favorable comparisons have been observed between the experimental information and the theoretical prediction, for both direct visualization of gas temperature pattern and temperature profile on the top and bottom walls.

(2) In the present configuration with horizontal mounting, the top wall temperature depicts a double-peak profile and the bottom wall temperature depicts a single-peak profile. These characteristics are caused by the interaction of the curvature of the high-temperature core between the two electrode tips and the curvature of the arctube. The curvature of the high-temperature core in the mercury gas field is largely dictated by the balance between the upward buoyancy effect and the electric field which tends to form a straight path to conduct the current between the electrodes.

(3) The inclination angle does not exert a large impact on the mercury gas temperature pattern in the mid-plane due to, again, the constraint of the electric field.

(4) The effects of the inclination angle on the tube wall temperature distribution are much more substantial than on the core gas temperature distribution due to the convection effect. The wall temperature not only shows a progressively more asymmetric distribution as the inclination angle increases, the gap between the highest and lowest wall temperatures also increases with the inclination angle. Hence the uniformity of the overall temperature field of the arctube worsens with non-horizontal mounting of the arctube.

(5) There exist noticeable differences between the measured and predicted lower wall temperature close to the end regions. Both the conduction and the radiation treatments of the present model, especially the latter, can be improved.

Acknowledgements—The authors wish to thank Mark Duffy and Pat Manney for providing the wall temperature measurements and the direct photographs. The helpful discussions held with Jim Dakin and Jack Strok on the modeling aspect are also gratefully acknowledged.

REFERENCES

1. W. Elenbaas, *Light Source*. Crane, Russak & Company, Inc., New York (1972).
2. R. J. Zollweg, Convection in vertical high-pressure mercury arcs, *J. Appl. Phys.* **49**, 1077–1091 (1978).
3. J. T. Dakin and W. Shyy, The prediction of convective and additive demixing in vertical metal halide discharge lamps, *J. Electrochem. Soc.* **136**, 1210–1215 (1989).
4. J. S. Turner, *Buoyancy Effects in Fluids*. Cambridge University Press, Cambridge (1973).
5. B. Gebhart, Y. Jaluria, R. L. Mahajan and B. Sammakia, *Buoyancy-induced Flows and Transport*. Hemisphere, Washington, DC (1988).
6. W. Shyy and J. T. Dakin, Three-dimensional natural convection in a high-pressure mercury discharge lamp, *Int. Commun. Heat Mass Transfer* **15**, 51–58 (1988).
7. P. Y. Chang, W. Shyy and J. T. Dakin, A study of three-dimensional natural convection in high-pressure mercury lamps—I. Parametric variations with horizontal mounting, *Int. J. Heat Mass Transfer* **33**, 483–493 (1990).
8. J. K. Lovin and A. W. Lubkowitz, User's manual for RAVFAC (a radiation view factor computer program), NASA CR-61321 (1969).

ETUDE DE LA CONVECTION NATURELLE TRIDIMENSIONNELLE DANS LES LAMPES A MERCURE A HAUTE PRESSION—II. PROFILS DE TEMPERATURE PARIETALE ET ANGLES D'INCLINAISON

Résumé—Un modèle tridimensionnel permet l'étude de la convection naturelle dans la décharge d'arc dans une vapeur à mercure à haute pression à l'intérieur d'un tube courbe. On résout les équations simultanées de quantité de mouvement, de continuité, d'énergie, de champ électrique et de transfert radiatif simplifié. On étudie les degrés d'uniformité de la distribution de température sur la paroi du tube, l'effet de l'angle d'inclinaison du tube (par rapport à la gravité) sur le mécanisme de transport et sur la distribution de température. On obtient de bons accords entre les prédictions et les mesures. On trouve que les distributions de température dans le plan médian sont à peu près insensibles à l'angle d'inclinaison. Néanmoins, la distribution de température pariétale montre une sensibilité nettement plus grande à l'angle d'inclinaison. Ce changement de comportement de la distribution de température pariétale a des effets importants sur les performances du tube d'arc.

UNTERSUCHUNG DER DREIDIMENSIONALEN NATÜRLICHEN KONVEKTION IN HOCHDRUCK-QUECKSILBERDAMPFLAMPEN—II. WANDTEMPERATURVERLÄUFE UND NEIGUNGSWINKEL

Zusammenfassung—Ein dreidimensionales Rechenmodell wird erstellt, um den Transport von Quecksilber durch natürliche Konvektion bei hohem Druck in einem gekrümmten Rohr, ausgehend von einem Lichtbogen, zu untersuchen. Das Modell beinhaltet Impulssatz, Kontinuitätsgleichung, Energiesatz, die Gesetze des elektrischen Feldes und vereinfachte Beziehungen für den Strahlungsaustausch. Im Rahmen dieser Arbeit wird untersucht, inwieweit das Temperaturfeld auf der Rohrwand ausgeglichen ist und welchen Einfluß der Neigungswinkel gegen die Vertikale auf die Transportvorgänge und die daraus resultierende Temperaturverteilung hat. Die Übereinstimmung zwischen Modellprognose und Messungen ist gut. Es stellt sich heraus, daß die Form des Temperaturfeldes im Gas in der Mittelebene kaum vom Neigungswinkel beeinflußt wird. Im Gegensatz dazu ist die Temperaturverteilung an der Wand stärker vom Neigungswinkel abhängig. Diese Änderung in der Temperaturverteilung an der Wand beeinflußt die Leistungsfähigkeit der Lichtbogenröhre erheblich.

ИССЛЕДОВАНИЕ ТРЕХМЕРНОЙ ЕСТЕСТВЕННОЙ КОНВЕКЦИИ В РТУТНЫХ ЛАМПАХ ВЫСОКОГО ДАВЛЕНИЯ—II. ПРОФИЛИ ТЕМПЕРАТУР СТЕНКИ И УГЛЫ НАКЛОНА

Аннотация—Для исследования естественной конвекции при дуговом разряде паров ртути высокого давления в изогнутой трубке использована трехмерная модель. Эта модель включает взаимосвязанные уравнения импульса, неразрывности, энергии, электрического поля и упрощенное уравнение радиационного переноса. В результате их решения получены степени однородности температурного распределения на стенке трубки и установлен характер влияния угла наклона трубки относительно вертикли на процессы переноса и результирующее температурное распределение. Обнаружено хорошее согласие расчетных данных с экспериментальными. Найдено, что результирующие распределения температуры газа в средней плоскости довольно незначительно зависят от угла наклона. Однако температурное распределение на стенке зависит от него гораздо сильнее. Это обстоятельство существенно влияет на рабочие характеристики дуговой лампы.